Published in final edited form as:
Science. 2016 July 08; 353(6295): 179–184. doi:10.1126/science.aaf6756.

Reengineering chimeric antigen receptor T cells for targeted therapy of autoimmune disease

Christoph T. Ellebrecht[1], **Vijay G. Bhoj**[2], **Arben Nace**[1], **Eun Jung Choi**[1], **Xuming Mao**[1], **Michael Jeffrey Cho**[1], **Giovanni Di Zenzo**[3], **Antonio Lanzavecchia**[4], **John T. Seykora**[1], **George Cotsarelis**[1], **Michael C. Milone**[2,†,*], and **Aimee S. Payne**[1,*,†]

[1]Department of Dermatology, University of Pennsylvania, Philadelphia, PA 19104, USA [2]Department of Pathology and Laboratory Medicine, University of Pennsylvania, Philadelphia, PA 19104, USA [3]Laboratory of Molecular and Cellular Biology, Istituto Dermopatico dell'Immacolata (IDI-IRCCS), 00167 Rome, Italy [4]Institute for Research in Biomedicine, 6500 Bellinzona, Switzerland

Abstract

Ideally, therapy for autoimmune diseases should eliminate pathogenic autoimmune cells while sparing protective immunity, but feasible strategies for such an approach have been elusive. Here, we show that in the antibody-mediated autoimmune disease pemphigus vulgaris (PV), autoantigen-based chimeric immunoreceptors can direct T cells to kill autoreactive B lymphocytes through the specificity of the B cell receptor (BCR). We engineered human T cells to express a chimeric autoantibody receptor (CAAR), consisting of the PV autoantigen, desmoglein (Dsg) 3, fused to CD137-CD3ζ signaling domains. Dsg3 CAAR-T cells exhibit specific cytotoxicity against cells expressing anti-Dsg3 BCRs in vitro and expand, persist, and specifically eliminate Dsg3-specific B cells in vivo. CAAR-T cells may provide an effective and universal strategy for specific targeting of autoreactive B cells in antibody-mediated autoimmune disease.

Pemphigus vulgaris (PV) is a life-threatening autoimmune blistering disease caused by autoantibodies to the keratinocyte adhesion protein Dsg3 (1). CD20-targeted B cell depletion results in short-term disease remission in 95% of pemphigus patients, but 81% relapse and fatal infection may occur (2). After CD20-targeted depletion, serum autoantibody titers drop, indicating that short-lived plasmablasts are the source of autoantibodies in PV and targeting of $CD20^+$ memory B cell precursors indirectly depletes autoantibody-secreting $CD20^-$ plasmablasts (3, 4). Relapsing pemphigus demonstrates the same anti-Dsg3 B cell clones observed during active disease, whereas disease remission is associated with disappearance

*Corresponding author. aimee.payne@uphs.upenn.edu (A.S.P.); milone@mail.med.upenn.edu (M.C.M.).
†These authors contributed equally to this work.

SUPPLEMENTARY MATERIALS
www.sciencemag.org/content/353/6295/179/suppl/DC1
Materials and Methods
Figs. S1 to S11
Table S1
Movies S1 and S2
References (38–55)

of circulating anti-Dsg3 B cells (5). Thus, targeted elimination of anti-Dsg3 memory B cells should cure PV without the risks of general immunosuppression.

Recently, chimeric antigen receptor (CAR) technology has revolutionized cancer therapy. A CD19-specific CAR, consisting of an extracellular single-chain variable fragment (scFv) antibody to CD19 fused to T cell cytoplasmic signaling domains, activates T cell cytotoxicity upon contact with $CD19^+$ B cells, causing specific and permanent elimination of B cells and durable remission of leukemia (6–14). In PV, pathogenic memory B cells express anti-Dsg3 B cell receptors (BCRs). We reasoned that by expressing Dsg3 as the extracellular domain of a chimeric immunoreceptor, cytotoxicity would become specific for only those B cells bearing anti-Dsg3 BCRs, providing targeted therapy for PV without general immunosuppression. Such a strategy would directly eliminate surface immunoglobulin $(sIg)^+$ anti-Dsg3 memory B cells and indirectly eliminate sIg^- Dsg3-specific short-lived plasma cells that produce the disease-causing antibodies. We thus created a chimeric autoantibody receptor (CAAR) (fig. S1A), with the autoantigen Dsg3 as the CAAR extracellular domain, in order to engineer T cells to kill autoimmune B cells in PV.

Dsg3 consists of five extracellular cadherin (EC) domains, with residues important for cell adhesion residing in EC1 and EC2 (15). Autoantibodies to EC1, EC2, EC3, EC4, and EC5 occur in 91, 71, 51, 19, and 12% of PV sera; no PV sera target only the EC4 and/or EC5 domains (16). Since T cell activation depends on the intermembrane distance of the immunologic synapse (17), we reasoned that shorter conformational fragments of Dsg3 should enhance CAAR efficacy. We therefore designed a panel of Dsg3 CAARs for expression in primary human T cells (Fig. 1A), using Dsg3 EC1-3/EC1-4/EC1-5 as the extracellular domain, fused to a dimerization-competent CD8α transmembrane (18) and CD137-CD3ζ cytoplasmic signaling domains, which were used successfully in CD19 CAR clinical trials (6, 7). EC1-3/EC1-4 CAARs demonstrate robust surface expression of mature, conformational Dsg3 in primary human T cells, whereas EC1-5 CAAR expression is more variable (fig. S1, B to D).

We first evaluated the ability of Dsg3 CAAR-T cells (CAAR-Ts) to kill anti-Dsg3 B cells in vitro, using antibody-secreting hybridomas that target EC1 (AK23), EC2 (AK19), and EC3-4 (AK18) (19), or K562/Nalm-6 cells expressing pathogenic F779/anti-EC1 or PVB28/anti-EC2 IgG cloned from PV patients (20, 21) (fig. S2). All BCRs were expressed at a density comparable to human B cells (fig. S3). Dsg3EC1-3/EC1-4 CAAR-Ts demonstrate interferon-γ (IFN-γ) secretion and specific cytolysis against anti-EC1/EC2 but not control targets (Fig. 1, B and C, and fig. S4). Dsg3EC1-5 CAAR-Ts exhibit minimal cytolysis, and Dsg3EC1-3 CAAR-Ts do not lyse anti-EC3/4 targets. Thus, the Dsg3EC1-4 CAAR demonstrates the best combination of potency and breadth, with specific cytolysis of cells expressing anti-Dsg3 BCRs.

To investigate the mechanism of CAAR-T activation, we examined the molecular organization within CAAR-Ts upon binding sIg target by total internal reflection fluorescence microscopy. CAAR-Ts form immunologic synapses analogous to T cell receptor (TCR)–peptide/major histocompatibility complex (MHC) interaction (22, 23), with

actin reorganization and centripetal movement of CAAR-IgG clusters resulting in a central supramolecular activation complex (SMAC)–like structure (fig. S5A and movie S1). The protein tyrosine phosphatase CD45 is excluded from early CAAR-IgG microclusters (fig. S5B and movie S2), similar to findings with the anti-CD19 CAR (24) and the native TCR-MHC synapse (25), suggestive of a kinetic segregation model for CAAR activation (26).

PV patients have serum anti-Dsg3 IgG that might neutralize, or alternatively could help stimulate, Dsg3 CAAR-Ts. We therefore evaluated Dsg3 CAAR-T cytotoxicity in the presence of soluble monoclonal IgG matching the targeted BCR to maximize the neutralization capacity of the soluble IgG. Soluble anti-Dsg3 IgG decreases but still preserves compelling CAAR-T cytotoxicity against AK19/PVB28, minimally affects AK23/AK18, and potentiates cytotoxicity against F779 targets (Fig. 2, A and B). Because CAAR-Ts will encounter polyclonal anti-Dsg3 IgG in PV patients, we next tested Dsg3 CAAR-T cytotoxicity against polyclonal targets in the presence of polyclonal PV serum IgG. Dsg3EC1-3, and to a lesser extent Dsg3EC1-4, CAAR-Ts retained efficient levels of cytolysis against AK hybridomas (Fig. 2C), despite the presence of PV serum IgG as well as secreted anti-Dsg3 IgG by these hybridomas. Both Dsg3EC1-3 and EC1-4 CAAR-Ts effectively killed Nalm6 cells expressing human anti-Dsg3 IgG in the presence of PV serum IgG (Fig. 2D). Surface binding competition assays indicate that antibodies that inhibit cytotoxicity (AK19/PVB28) persist on the CAAR-T surface, which reduces the number of accessible CAAR molecules to bind target cells, while noninhibitory F779/AK23/AK18 are more rapidly replaced by competing antibodies, with AK18 replacement occurring even at 4°C, suggesting low affinity (Fig. 2, E and F). Indeed, surface plasmon resonance analysis indicates that noninhibitory antibodies tend to have faster off-rates and lower affinity (Fig. 2, G and H, and fig. S6A). Furthermore, F779 and PV serum IgG stimulate Dsg3EC1-4 CAAR-Ts, more so than the Dsg3EC1-3 CAAR-Ts, to secrete low levels of IFN-γ and proliferate (fig. S6, B and C). Thus, the effect of soluble antibodies to Dsg3 on CAAR-T function and activation is a complex process that is affected by affinity and binding kinetics of the antibody, as well as the relative position of the epitope in the CAAR molecule, highlighted by the different susceptibility of the EC1-3 and EC1-4 CAARs to blockade and activation. Collectively, these data suggest that soluble anti-Dsg3 IgG will not prevent and may in fact promote CAAR-T efficacy and persistence due to CD137-mediated costimulatory signals that have been shown to enhance CAR-T activity (27–30) and ameliorate T cell exhaustion (31).

We tested the in vivo efficacy of Dsg3 CAAR-Ts against AK23/AK19/AK18 target cells in a PV mouse model (19). We selected the PV hybridoma model for in vivo proof of concept, because this model allows preclinical testing of human Dsg3 CAAR-T efficacy against B cells targeting distinct and defined Dsg3 epitopes. Furthermore, the mice have polyclonal serum anti-Dsg3 IgG (like PV patients) that might neutralize or eliminate CAAR-Ts, and disease burden can be serially and objectively quantitated by bioluminescence imaging. NSG (NOD-scid-gamma) mice were injected with a polyclonal mixture of bioluminescent AK18/AK19/AK23 hybridomas, followed by injection with either Dsg3 CAAR-Ts or control CAR-Ts at day 5 (fig. S7A), at which time serum antibody titers to Dsg3 were detectable by enzyme-linked immunosorbent assay (ELISA) (Fig. 3A). Dsg3 CAAR-Ts robustly control all PV hybridomas, resulting in decreased Dsg3 serum autoantibody titers

(Fig. 3A), absence of autoantibody binding (Fig. 3B) and blistering in oral mucosa (Fig. 3C), and significantly delayed or no hybridoma outgrowth (Fig. 3D). Dsg3EC1-4 CAAR-Ts showed equal efficacy when tested against each individual hybridoma in vivo (fig. S8, A to G). We further analyzed a subset of Dsg3EC1-4 CAAR-T–treated mice with increasing bioluminescence at day 18. Increasing flux was due to outgrowth of sIg^- hybridomas that comprised ~1% of injected cells (fig. S8, H to J). This mechanism of CAAR-T escape observed in mice is irrelevant in patients because sIg^- long-lived plasma cells do not significantly contribute to PV autoantibody production. Dsg3 CAAR-T frequencies in both "escape" and "cured" mice were comparable, indicating that lack of CAAR-T cell persistence or loss of Dsg3 CAAR expression is not responsible for CAAR escape in vivo (fig. S8K).

We further tested the in vivo efficacy of Dsg3EC1-4 CAAR-Ts against human $CD19^+$ Nalm-6 B cells expressing anti-Dsg3 BCRs (F779/PVB28) cloned from PV patients. This model additionally allows comparison with anti-CD19 CAR-Ts (CART19) that have proven clinical efficacy (6, 7). Although CAAR-T treatment is delayed until the exponential growth phase of the target cells, Dsg3 CAAR-Ts effectively eliminate anti-Dsg3 Nalm-6 B cells with efficacy comparable to CART19, measured by bioluminescence and flow cytometric analysis of bone marrow/spleen (Fig. 3, E to G, and fig. S7, B and C). Collectively, these models show that Dsg3 CAAR-Ts eliminate anti-Dsg3 BCR^+ but not BCR^- cells in vivo, indicating specific cytolysis, as opposed to bystander activation and off-target cytolysis, even in the presence of soluble anti-Dsg3 IgG. Notably, CAAR-Ts persist in the presence of soluble autoantibodies to Dsg3 in vivo (fig. S8K), indicating that circulating autoantibodies do not cause Fc-mediated clearance of CAAR-Ts. Furthermore, CAAR-Ts showed engraftment and persistence in the spleen 3 weeks after CAAR-T transfer, even in the absence of target cells (fig. S8L), suggesting that persistence of CAAR-Ts does not depend on target cell encounter.

We next addressed CAAR-T safety by evaluating off-target effects against keratinocytes, which express desmocollins and desmogleins, the physiologic binding partners of Dsg3. The Dsg3CAAR does not exhibit CD3ζ-mediated signaling in reporter cells after incubation with keratinocytes (Fig. 4, A and B), in contrast to positive control anti-Dsg3/1 (Px44) CAR. Correspondingly, Dsg3EC1-4 CAAR-Ts do not lyse human keratinocytes in vitro, whereas Px44 CAR-Ts show potent lysis (Fig. 4C). To evaluate toxicity in vivo, we tested CAAR-Ts in human skin-xenografted mice (Fig. 4D). Px44 CAR-Ts exhibit exuberant epidermal infiltration by day 3 (Fig. 4, D and E). Despite similar T cell density in the graft dermis, Dsg3EC1-4 CAAR-Ts do not demonstrate enhanced skin toxicity compared with CART19, which has shown no skin side effects in humans. Additionally, no off-target toxicity against other tissues was observed in Dsg3EC1-4 CAAR-T–treated mice (fig. S9). Because human Dsg3 rescues the loss of mouse Dsg3, indicating functional interaction between human Dsg3 and mouse desmosomal components (32), these experiments indicate that Dsg3EC1-4 CAAR-Ts cause no toxicity to desmosome-bearing tissues in vivo. The absence of off-target toxicity to desmosome-bearing tissues might be explained by several factors. The intermembrane distance in desmosomes is 35 nm (15), greater than the 15-nm optimum distance for T cell activation. Additionally, cadherin-cadherin affinity is in the micromolar range (33), whereas CAR-T function typically requires nanomolar affinity (34–36). Finally,

Dsg3 truncation (EC1-3/EC1-4) potentially compromises CAAR interaction with desmosomal ligands while preserving epitopes required for autoantibody binding, thus preventing off-target toxicity.

We also considered that FcγR-expressing cells bind serum antibodies to Dsg3 and might become targets for Dsg3 CAAR-Ts, although significant toxicity is unlikely because anti-Dsg3 IgG comprises only a small fraction of total serum IgG. In the presence of PV serum, cytotoxicity against $CD64^+$ ($Fc\gamma R^+$) K562 cells was undetectable (fig. S10, A and B). Additionally, Dsg3EC1-4 CAAR-T treatment in the setting of circulating anti-Dsg3 IgG does not reduce FcγR-expressing cells such as neutrophils and monocytes in vivo (fig. S10C), indicating that redirected killing via CAAR-antibody-FcγR interaction does not occur. Furthermore, CAAR-T reporter cells do not activate when exposed to bone marrow B cells that harbor a polyreactive and/or autoreactive repertoire (37), in contrast to CART19, which reacts with bone marrow B cells (fig. S11). Thus, toxicity by Dsg3EC1-4 CAAR-Ts is undetectable, underscoring the specificity of the CAAR concept.

In summary, CAAR-Ts represent a targeted approach to therapy of antibody-mediated autoimmune diseases, with the potential for generation of long-term memory CAAR-Ts that can potentially cure disease. CAAR-Ts expressing the PV autoantigen Dsg3 specifically kill anti-Dsg3 target cells, even in the presence of circulating autoantibodies, and without off-target toxicity. We acknowledge that short-term observations of CAAR-T safety and efficacy in preclinical models are inherently limited. Nevertheless, several of the limitations of CAR-T therapy for cancer likely will not apply to CAAR-T therapy of autoimmunity. Target cell escape due to epitope spreading or somatic mutation is impossible, because B cells that no longer bind Dsg3 will become irrelevant to disease. Additionally, memory B cells depend on survival and activation signals through the BCR; thus, anti-Dsg3 B cells that down-regulate sIg are unlikely to persist or mature into antibody-secreting cells. Tumor lysis and cytokine release syndrome are also unlikely since Dsg3-reactive B cells are predicted to comprise only a small fraction of the total B cell population. Ultimately, various combinations of CAARs could be combined to maximize efficacy in diseases in which autoantibodies targeting multiple autoantigens are pathogenic. Thus, CAAR-T cells represent an innovative therapeutic strategy that avoids the risks of general immunosuppression and can likely be applied to other autoantibody-mediated diseases.

Supplementary Material

Refer to Web version on PubMed Central for supplementary material.

Acknowledgments

We thank D. Margolis, S. Prouty, T. Dentchev, C.-Y. Tsai, and S. Nunez-Cruz for technical assistance and consultation on the studies and J. R. Stanley for helpful discussions. The data reported in this manuscript are tabulated in the main paper and in the supplementary materials. Constructs and cell lines are available from the corresponding authors under a Material Transfer Agreement with the University of Pennsylvania. C.T.E., V.G.B., M.C.M, and A.S.P. have filed patent PCT/US15/28872, 2015, which relates to compositions and methods of chimeric autoantibody receptor T cells. C.T.E. and A.S.P. have filed Provisional Patent Application 62/222,132, 2015, which relates to the VRC01 chimeric antigen receptor. Research reported in this publication was supported in part by the Penn Institute for Immunology (A.S.P. and M.C.M.); the Dermatology Foundation Charles and Daneen Stiefel Scholar Award (A.S.P.); the National Institute of Arthritis and Musculoskeletal and Skin Diseases of NIH

(A.S.P., R01-AR057001 and R01-AR068288; M.J.C., T32-AR007465 and F31-AR066456; G.C., R01-AR055309; and Skin Diseases Research Core grant P30-AR057217); Deutsche Forschungsgemeinschaft (C.T.E., EL711/1-1); the National Cancer Institute of NIH (V.G.B., T32-CA009140); the National Heart, Lung, and Blood Institute of NIH (V.G.B., K12-HL087064); and the Italian Ministry of Health (G.D.Z., Ricerca Finalizzata RF10-2309790). The content is solely the responsibility of the authors and does not necessarily represent the official views of the National Institutes of Health.

REFERENCES AND NOTES

1. Payne, AS., Stanley, JR. Dermatology in General Medicine. Wolff, K., et al., editors. Vol. chap. 53. McGraw Hill; New York: 2012.
2. Colliou N, et al. Sci Transl Med. 2013; 5:175ra30.
3. Eming R, et al. J Invest Dermatol. 2008; 128:2850–2858. [PubMed: 18563178]
4. Lunardon L, et al. Arch Dermatol. 2012; 148:1031–1036. [PubMed: 22710375]
5. Hammers CM, et al. J Invest Dermatol. 2015; 135:742–749. [PubMed: 25142730]
6. Porter DL, Levine BL, Kalos M, Bagg A, June CH. N Engl J Med. 2011; 365:725–733. [PubMed: 21830940]
7. Maude SL, et al. N Engl J Med. 2014; 371:1507–1517. [PubMed: 25317870]
8. Davila ML, et al. Sci Transl Med. 2014; 6:224ra25.
9. Lee DW, et al. Lancet. 2015; 385:517–528. [PubMed: 25319501]
10. Kochenderfer JN, et al. J Clin Oncol. 2015; 33:540–549. [PubMed: 25154820]
11. Brentjens RJ, et al. Blood. 2011; 118:4817–4828. [PubMed: 21849486]
12. Cruz CR, et al. Blood. 2013; 122:2965–2973. [PubMed: 24030379]
13. Savoldo B, et al. J Clin Invest. 2011; 121:1822–1826. [PubMed: 21540550]
14. Turtle CJ, et al. J Clin Invest. 2016; 126:2123–2138. [PubMed: 27111235]
15. Al-Amoudi A, Díez DC, Betts MJ, Frangakis AS. Nature. 2007; 450:832–837. [PubMed: 18064004]
16. Ohyama B, et al. J Invest Dermatol. 2012; 132:1158–1168. [PubMed: 22277941]
17. Choudhuri K, Wiseman D, Brown MH, Gould K, van der Merwe PA. Nature. 2005; 436:578–582. [PubMed: 16049493]
18. Hennecke S, Cosson P. J Biol Chem. 1993; 268:26607–26612. [PubMed: 8253791]
19. Tsunoda K, et al. J Immunol. 2003; 170:2170–2178. [PubMed: 12574390]
20. Di Zenzo G, et al. J Clin Invest. 2012; 122:3781–3790. [PubMed: 22996451]
21. Cho MJ, et al. Nat Commun. 2014; 5:4167. [PubMed: 24942562]
22. Monks CRF, Freiberg BA, Kupfer H, Sciaky N, Kupfer A. Nature. 1998; 395:82–86. [PubMed: 9738502]
23. Grakoui A, et al. Science. 1999; 285:221–227. [PubMed: 10398592]
24. James JR, Vale RD. Nature. 2012; 487:64–69. [PubMed: 22763440]
25. Varma R, Campi G, Yokosuka T, Saito T, Dustin ML. Immunity. 2006; 25:117–127. [PubMed: 16860761]
26. Davis SJ, van der Merwe PA. Nat Immunol. 2006; 7:803–809. [PubMed: 16855606]
27. Melero I, et al. Nat Med. 1997; 3:682–685. [PubMed: 9176498]
28. Ye Z, et al. Nat Med. 2002; 8:343–348. [PubMed: 11927939]
29. Yang S, et al. Proc Natl Acad Sci USA. 2004; 101:4990–4995. [PubMed: 15051893]
30. Zhao Z, et al. Cancer Cell. 2015; 28:415–428. [PubMed: 26461090]
31. Long AH, et al. Nat Med. 2015; 21:581–590. [PubMed: 25939063]
32. Culton DA, et al. J Invest Dermatol. 2015; 135:1590–1597. [PubMed: 25695683]
33. Katsamba P, et al. Proc Natl Acad Sci USA. 2009; 106:11594–11599. [PubMed: 19553217]
34. Hudecek M, et al. Clin Cancer Res. 2013; 19:3153–3164. [PubMed: 23620405]
35. Watanabe K, et al. Blood. 2014; 124:4799.
36. Srivastava S, Riddell SR. Trends Immunol. 2015; 36:494–502. [PubMed: 26169254]

37. Wardemann H, et al. Science. 2003; 301:1374–1377. [PubMed: 12920303]

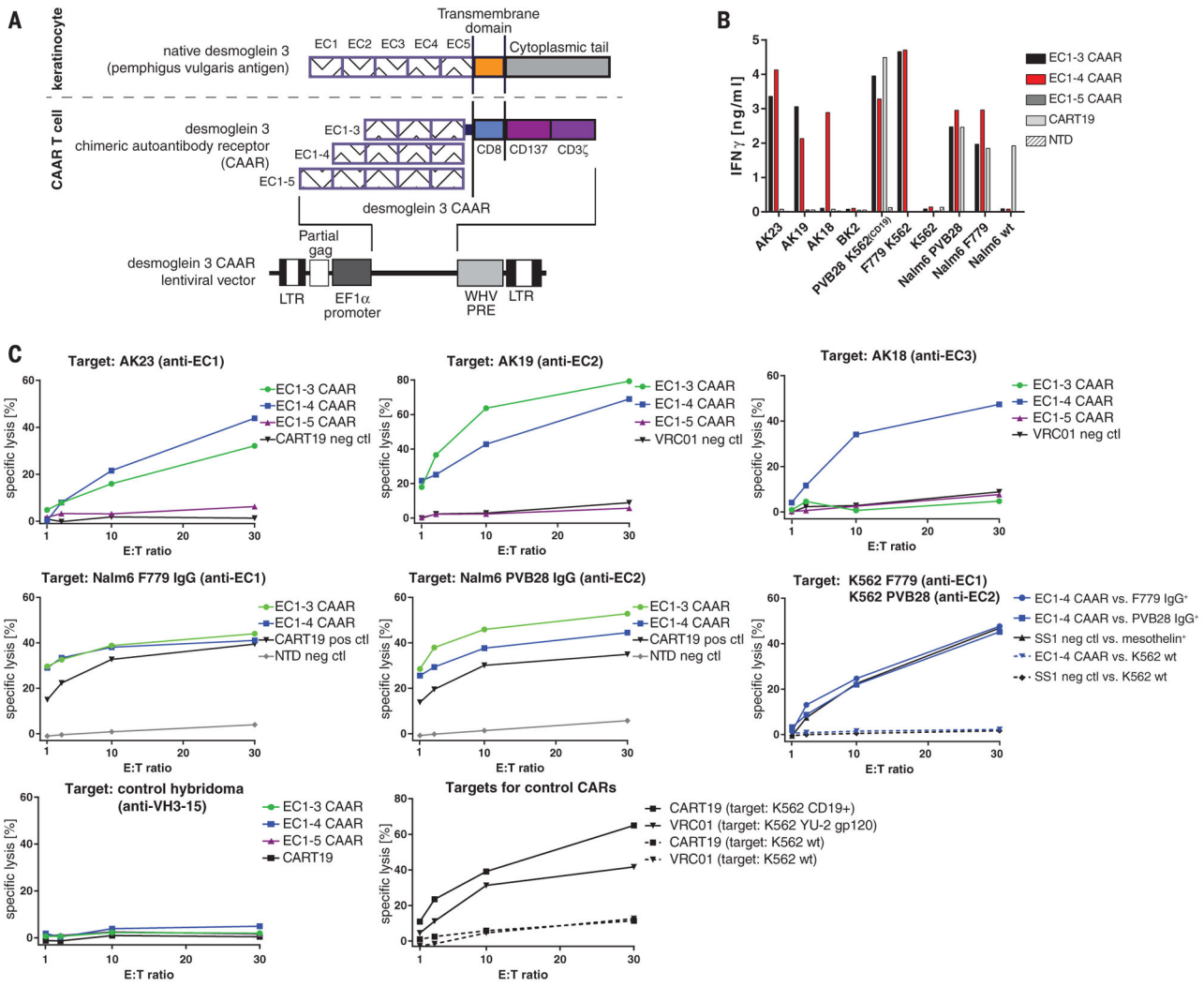

Fig. 1. Dsg3 CAAR-T cells demonstrate specific and potent cytotoxicity

(**A**) Schematic of native Dsg3, Dsg3 CAAR, and lentiviral vector for stable CAAR expression. (**B**) Specific IFN-γ production by CAAR-Ts as measured by ELISA from coculture supernatant after 24 hours. Cultures were set up in duplicate; mean values are shown. Similar results were obtained in independent experiments from at least five different healthy Tcell donors. (**C**) ^{51}Cr release after 4 hours of Tcell–target cell coculture at indicated effector to target (E:T) ratios to measure specific cytotoxicity by Dsg3 CAAR-Ts against distinct anti-Dsg3 target cells. Mean values of triplicate cultures are shown. Similar results were obtained in independent experiments from at least five different healthy Tcell donors.

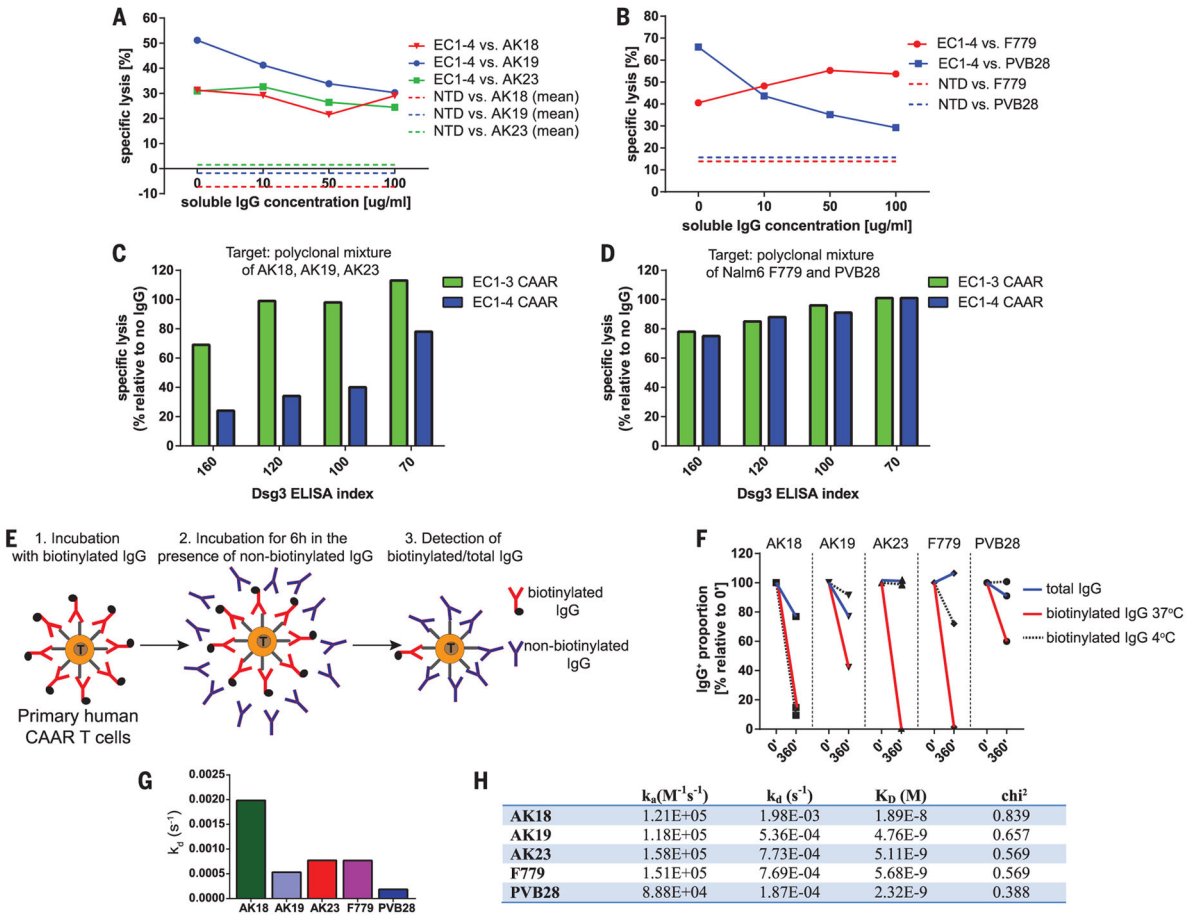

	k_a($M^{-1}s^{-1}$)	k_d (s^{-1})	K_D (M)	chi²
AK18	1.21E+05	1.98E-03	1.89E-8	0.839
AK19	1.18E+05	5.36E-04	4.76E-9	0.657
AK23	1.58E+05	7.73E-04	5.11E-9	0.569
F779	1.51E+05	7.69E-04	5.68E-9	0.569
PVB28	8.88E+04	1.87E-04	2.32E-9	0.388

Fig. 2. Dsg3 CAAR-Tcells maintain cytotoxicity in the presence of soluble antibodies to Dsg3

(**A** to **D**) ^{51}Cr release after 4 hours of T cell–target cell coculture at an E:T ratio of 30:1 to measure specific cytotoxicity by Dsg3 CAAR-Ts in the presence of [(A) and (B)] soluble, monoclonal antibodies to Dsg3 at indicated concentrations or [(C) and (D)] soluble, polyclonal antibodies to Dsg3 at indicated Dsg3 ELISA indices. Mean values from triplicate cultures are shown. Results are representative of two independent experiments with CAAR-T cells from two different donors. (**E**) Experimental setup for pulse-chase antibody cell-surface binding assay. (**F**) Total surface IgG and retained biotinylated IgG were detected by flow cytometry after 6 hours of culture with excess nonbiotinylated IgG at 4°C and 37°C to assess the blocking property of soluble IgG toward each B cell clone. Similar results were replicated in three independent experiments with Dsg3EC1-4 CAAR-T cells from three different T cell donors. (**G** and **H**) Surface plasmon resonance demonstrating higher off-rates (k_d) and lower affinity (higher K_D) of nonblocking antibodies AK18, AK23, and F779. Values were calculated from four different concentrations, as indicated in fig. S6A.

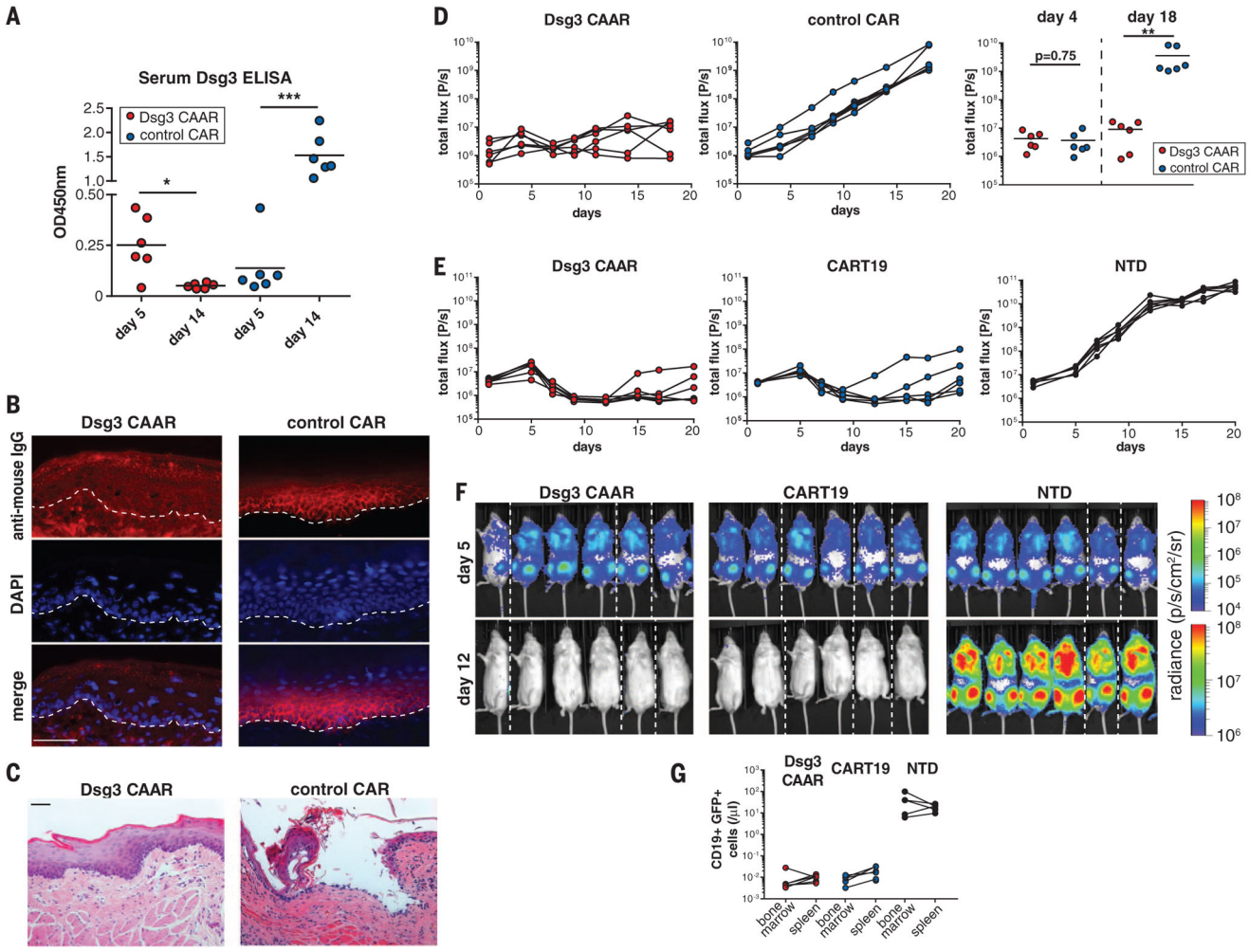

Fig. 3. Dsg3 CAAR-T cells eliminate anti-Dsg3 target cells in vivo

(**A**) Serum anti-Dsg3 ELISA was performed on days 5 and 14 to quantify IgG production by hybridoma cells before and after CAAR-T treatment. Paired *t* test, two-tailed; $*P < 0.05$; $***P < 0.001$. (**B**) Direct immunofluorescence of mucosa samples to detect IgG deposition after CAAR-T or control Tcell treatment. Absence of IgG deposition was seen in all CAAR-T–treated mice. (**C**) Histologic mucosal blister formation (i.e., acantholysis) was assessed after CAAR-T treatment. None of six CAAR-T–treated mice, versus five of six control Tcell–treated mice, demonstrated acantholysis; $P = 0.015$, Fisher's exact test. Scale bars in (B) and (C), 50 µm. (**D**) Serial quantification of hybridoma burden by bioluminescence imaging. Unpaired Mann-Whitney test, two-tailed, $**P < 0.01$; results were replicated in an independent experiment with Tcells from a different donor. Symbols represent one mouse each; horizontal black lines represent the mean of each group. (**E**) Bioluminescence imaging quantification of Nalm6 $CD19^+$ B cells expressing PVB28/F779 IgG after Dsg3 CAAR-T, anti-CD19 CAR-T (CART19), or nontransduced Tcell (NTD) treatment. (**F**) Bioluminescence on days 5 and 12 after Nalm6 injection. Dashed lines separate images from different cages. (**G**) Flow cytometric quantification of Nalm6 cells in bone marrow and spleen in the three treatment groups 22 days after Nalm6 injection.

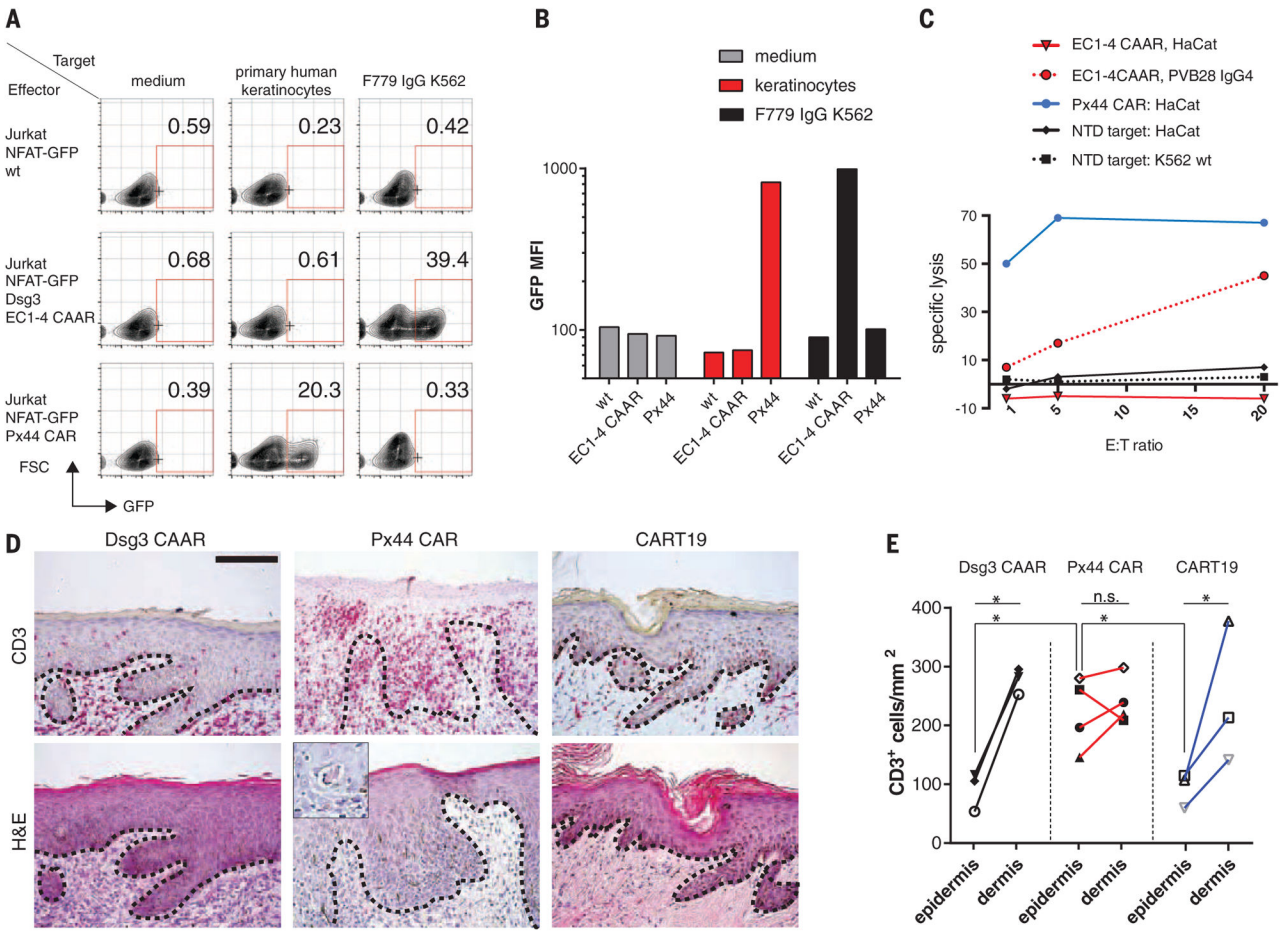

Fig. 4. Dsg3 CAAR-Tcells do not showoff-target toxicity

(**A**) Flow-cytometric quantification of CAAR-mediated signal transduction, as indicated by nuclear factor of activated Tcells (NFAT)–driven green fluorescent protein (GFP) expression in Jurkat reporter cells, using anti-Dsg3/1 Px44 CAR as a positive control for keratinocyte expression of Dsg3. Numbers indicate percentage of live, single cells in the GFP-positive gate. (**B**) Mean fluorescence intensity of GFP expression from (A). Representative data were replicated in at least five independent experiments with keratinocytes from different human donors. (**C**) ^{51}Cr release after T cell–target cell coculture at indicated E:T ratios to measure cytotoxicity by Dsg3 CAAR-Ts and controls against human HaCat keratinocytes. Mean values of triplicate cultures are shown; similar results were obtained in two independent experiments. (**D**) Microscopic analysis of human skin xenografts to evaluate epidermal infiltration by Dsg3CAAR-Ts, positive control Px44 CAR-Ts, and negative control CART19. (Inset) Dyskeratotic keratinocytes surrounded by T cells. Dashed line shows dermal-epidermal junction. Scale bar, 125 μm. (**E**) Quantification of T cell infiltration into epidermis and dermis of human skin xenografts. Each symbol represents one mouse; ratio-paired *t* test, two-tailed, $*P < 0.05$; n.s. nonsignificant; data are pooled from two independent experiments.